Arabian Journal for Science and Engineering (2023) 48:341–351
https://doi.org/10.1007/s13369-022-07031-w

RESEARCH ARTICLE-CHEMISTRY

# Characterization, Properties and Antimicrobial Activity of Radiation Induced Phosphorus-Containing PVA Hydrogels

**H. L. Abd El-Mohdy[1] · Hala M. Aly[2]**

Received: 14 November 2021 / Accepted: 5 June 2022 / Published online: 20 July 2022


**Abstract**
Function modification of polyvinyl alcohol (PVA) having phosphorus-containing heterocyclic compounds is believed to have thermal and biological applications in the area of polymers. The synthesis of phosphorus-containing PVA (P-PVA) was performed using γ-radiation. The chemical structure of the composite polymer is confirmed by spectroscopic techniques of FT-IR, $^{1}$H, $^{13}$C, and $^{31}$P-NMR. Photosensitive properties of polymers were investigated by ultraviolet spectroscopy. Thermal studies are assigned using the Differential Scanning Calorimeter (DSC) and thermogravimetric analysis (TGA). Data display that P-PVA has more thermal stability than PVA. The surface morphology of the prepared hydrogels was performed using scanning electron microscopy (SEM). Quantitative elemental analysis of the P-PVA hydrogel was done through energy-dispersive X-ray spectroscopy (EDX). Antimicrobial activity of the prepared hydrogels using different fungi such as *Aspergillus fumigatus, Geotrichum candidum, Candida albicans,* and *Syncephal-astrum racemosum,* in addition to bacteria such as *Staphylococcus aureus, Bacillis subtilis* (as gram-positive bacteria), *Pseudomonas aeruginosa,* and*Escherichia coli* (as gram-negative bacteria), was studied. The phosphorus-contained PVA hydrogels were found to have antimicrobial activity against various fungi and bacteria compared to pure PVA hydrogels.

**Keywords** Polyvinyl alcohol · Phosphorus-containing polymer · Radiation · Thermal studies · Antimicrobial activity

## 1 Introduction

For more than 30 years researchers have begun to expose polymers to high-energy radiation such as gamma and electron beam cross-linking, coupling, and compliance [1]. High-strength polymers are gaining popularity in a wide range of high-performance applications due to the few advantages after polymers heating. The polymer-connected polymer at a prepared dose shows a better structural improvement compared to chemical reactions. As radiation processing is very simple, clean, non-toxic, and environmentally friendly compared to peroxide crosslinking and ethylene oxide sterilization. Both the combination of polymer and compound plays its role in attracting the attention of industrialists, scholars, and researchers of many applications [2–4]. The polymer mixed with radiation in controlled doses shows many advantages of structural improvements such as better mechanical strength, high thermal insulation, electrical insulation, chemical resistance, radiation resistance, and antimicrobial properties [5–7].

Polyvinyl alcohols (PVA) have garnered much interest over the years due to their vast range of applications. PVA is a material where physicochemical properties are dependent on the degree of polymerization, hydrolysis, and distribution of its hydroxyl groups. PVA is a suitable polymer to be used as a material for drug delivery, wound dressings, films, membranes, cancer cells, microcapsules, and hydrogel fixation; this is due to its decomposition, and water solubility, good biocompatibility, and non-toxicity [8–10]. PVA hydrogels produced by radiation are free of crosslinkers and therefore have high purity and good optical transparency. At the same time, high-energy reaction conditions often cause the loss of mechanical properties and other aspects. Another advantage of PVA hydrogels prepared by radiation crosslinking is that the reaction is rapid and can be achieved at room temperature and atmospheric pressure [11, 12]. However, due to radiation intensity, many materials cannot be added to the hydrogel

✉ H. L. Abd El-Mohdy
hatem_lotfy@yahoo.com

[1] National Center for Radiation Research and Technology (NCRRT), Egyptian Atomic Energy Authority, Cairo, Egypt

[2] Department of Chemistry, Faculty of Science (Girls), Al-Azhar University, Nasr City, Cairo, Egypt

systems. The antibacterial materials of the PVA hydrogel systems are generally expensive, and the modification methods are complicated. Therefore, the preparation of antibacterial PVA hydrogels with low cost and simple preparation, the large-scaled production method is the research focus [13]. The modification of PVA by introducing functional groups is believed to have a fundamental value in increasing its use. Many research articles have reported polymer modification by introducing carboxylic, sulfonate, and amino groups [14]. The combination of PVA-containing phosphorus and heteroaromatics in the main series attracts the attention of many researchers because of their unusual properties such as thermal stability, non-combustion, high melting points, and desirable biological functions [15].

Microbial infection is still one of the most serious problems associated with the use of indoor medical devices. Antimicrobial agents are those that can kill pathogenic microorganisms. In general, they are low-molecular-weight compounds. However, most of these molecules are toxic to the environment and their use is short-lived. If these materials are attached to polymers, it may be an ideal solution to overcome the problems associated with low molecular weight material. Many recent studies have focused on the development of antimicrobial polymers for high-value products [16–18]. Phosphorus-containing polymers are attractive antimicrobial compounds and some of them have shown enhanced antimicrobial activity compared to other polymers. Xu et al. synthesized a new poly [bis (octafluoropentoxy) phosphazene] (OFP) for the purpose of making blood contact with medical equipment. The data suggested that OFP textured materials could provide a practical way to improve the biocompatibility of current organisms in the use of blood in contact with medical equipment by significantly reducing the risk of pathogenic infections and thrombosis [19]. Somasundarana and Guhanathan [15] mentioned that bacterial activity improved due to phosphorus ingestion heterocyclic moieties in PVA. They proved that organophosphorus heterocyclic functionalized vinyl polymer was considered suitable for *Bacillus cereus, Staphylococcus aureus*, and *Escherichia coli*.

The aim of the present study is to synthesize phosphorus-containing heterocyclic-based polymers by reaction of PVA with heterocyclic compounds and phosphorus oxychloride to behave antimicrobial activity against various microbes. The properties of phosphorus-containing polymers such as thermal (DSC-TGA), spectral (UV, FTIR, and NMR), and biological activities have been investigated.

## 2 Experimental

### 2.1 Materials

Polyvinyl alcohol of purity 99%, pyridine, phosphorus oxychloride, 6-chlorobenzo[d]oxazol-2(3H)-one, and tetra hydro furan (THF) were used as received and purchased from Merck Co., Germany.

### 2.2 Preparation of N-Heterocyclic Phosphonyl Dichloride Moieties

About 0.068 g of 6-chlorobenzo[d]oxazol-2(3H)-one and 0.153 g of phosphorus oxychloride were dissolved separately in 20 mL of THF and added slowly over the other using an additional funnel with constant stirring for 15 min at 0 °C in the presence of a catalytic amount of pyridine. The reaction was continued for 3 h. Then the reaction mixture was filtered, and the solvent was evaporated to get 6-chloro-2-oxobenzo[d]oxazol-3(2H)-ylphosphonic dichloride.

### 2.3 Synthesis of Phosphorus-Containing Polymer

Crosslinked PVA was prepared by using a $^{60}$Co source supplied by National Center for Radiation Research and Technology, Egyptian Atomic Energy Authority. A previously prepared hetero-phosphorus compound; 6-chloro-2-oxobenzo[d]oxazol-3(2H)-ylphosphonic dichloride (1 mmol) and crosslinked PVA (0.6 g) were dissolved in 50 mL of dry DMF at 90 °C for 12 h with constant stirring. Then the solvent was removed under reduced pressure, and the resulting product was dried at 50 oC using a vacuum oven.

### 2.4 Gel Content

Hydrogels are dried and diluted with pure water for 24 hours at 100 °C to remove the insoluble parts of the hydrogel. The insoluble parts or gelled parts were extracted and washed with hot distilled water to remove the soluble parts and then dried and weighed. The various extraction stages were repeated until the weight fluctuated. The production of hydrogel gel is determined as follows:

$$\text{Gel}\ (\%) = (W_e/W_d) \times 100 \quad (1)$$

where $W_d$ and $W_e$ represent the weights of the dry hydrogel and the gelled part after extraction, respectively [20].

### 2.5 Swelling Measurement

Dried hydrogel disks (0.4–0.5 mm thickness, 5 mm diameter) are left to swell in distilled water. The swollen gel was periodically removed from the swollen area and dried slightly with a filter paper, then weighed and placed in the same tub. The measurements continued until a constant weight was reached [21].

$$\text{Swelling } \% = (W_s - W_d / W_d) \times 100 \quad (2)$$

where $W_s$ and $W_d$ represent the weights of swollen and dry samples, respectively. To study the kinetics of the water-sorption mechanism, the water–intake process was monitored by the determination of the hydrogel swelling ratio at desired time intervals as previously described.

### 2.6 Antimicrobial Assay

In this study, four bacteria and four fungi were used as test microorganisms. Test fungi include *Aspergillus fumigatus* (RCMB 002,003)*, Geotrichum candidum (RCMB 052,006), Candida albicans (RCMB 005,002),* and*Syncephalastrum racemosum (RCMB 005,003)* on Sabourad dextrose agar plates. Test bacteria include *Staphylococcus aureus* (RCMB 000106) and *Bacillus subtilis* (RCMB 000107) (as gram-positive bacteria) while *Pseudomonas aeruginosa* (RCMB 000102) and *Escherichia coli* (RCMB 000103) (as gram-negative bacteria). All strains have been supplemented by the Regional Center for Mycology and Biotechnology, Al-Azhar University, Cairo, Egypt. The medium used for growing bacteria was universal nutrient agar while Sabouraud and/or yeast malt extract agar were used for fungi [22]. Antimicrobial activity is determined by the agar well diffusion method. Agar plates are seeded with test microorganisms and kept for 30 min until the medium is hardened. Round 5 mm diameter pieces of the tested hydrogels were added. Plates are kept for 2 h at 4 °C before incubating at room temperature for bacteria or fungi. Plates were examined on daily basis for the development of growth inhibition zones around the loaded hydrogels.

### 2.7 Characterization

#### 2.7.1 Thermogravimetric Analysis

A Shimadzu TGA-50 system is used to study the thermal stability of the prepared copolymers under a nitrogen atmosphere. The temperature range is from the ambient temperature to 600 °C at a heating rate of 10 °C/min.

#### 2.7.2 Differential Scanning Calorimetry

The thermal parameters of hydrogels such as melting temperature (*Tm*) and heat of melting ($\Delta Hm$) are determined by DSC on a PerkinElmer apparatus equipped with a DSC-7 data station. For DSC measurements, about 5 mg specimen of the sample is used. The measurements were taken in a nitrogen atmosphere at a heating rate of 10 °C/min.

#### 2.7.3 Scanning Electron Microscopy

The lyophilized dried hydrogels were examined with a Jeol JSM-5400 SEM. The surfaces of the polymers were sputter-coated with gold for 3 min.

#### 2.7.4 NMR Spectral Analysis

NMR spectral analysis such as $^{31}$P NMR $^{13}$C NMR and $^{1}$H NMR for the prepared hydrogel samples was conducted on a DMX 500 spectrometer (Bruker Co., Germany) at room temperature with $D_2O$ as the solvent.

#### 2.7.5 EDX Measurements

Phosphorus and various elements are seen on EDX Oxford (England)—ISIS attached to SEM-JEOL-5400 with a voltage of 20 keV.

## 3 Results and Discussion

### 3.1 Synthesis of Phosphorus-Containing PVA

In this study, phosphorus–contained polymers in the main chain were synthesized. The method and strategy for the manufacture of the desired polymers from simple startup materials are mentioned here, Schemes 1 and 2. The structures of these products were confirmed by IR, and NMR spectroscopic analysis, and the thermal properties of these polymers were analyzed by DSC and TGA. The optical properties involving the absorption and luminescence of these polymers are measured with UV ± Vis systems. The photograph of neat PVA and phosphorus–contained polymers; P-PVA is shown in Fig. 1. There is a difference in hydrogel color between the two hydrogel samples. PVA has a light color whereas; P-PVA has a dark color.

### 3.2 FT-IR and NMR Analysis

The chemical properties of the resulting polymers were confirmed by FT-IR and spectroscopic NMR analysis. As shown in Fig. 2, the current FT-IR spectra of the system

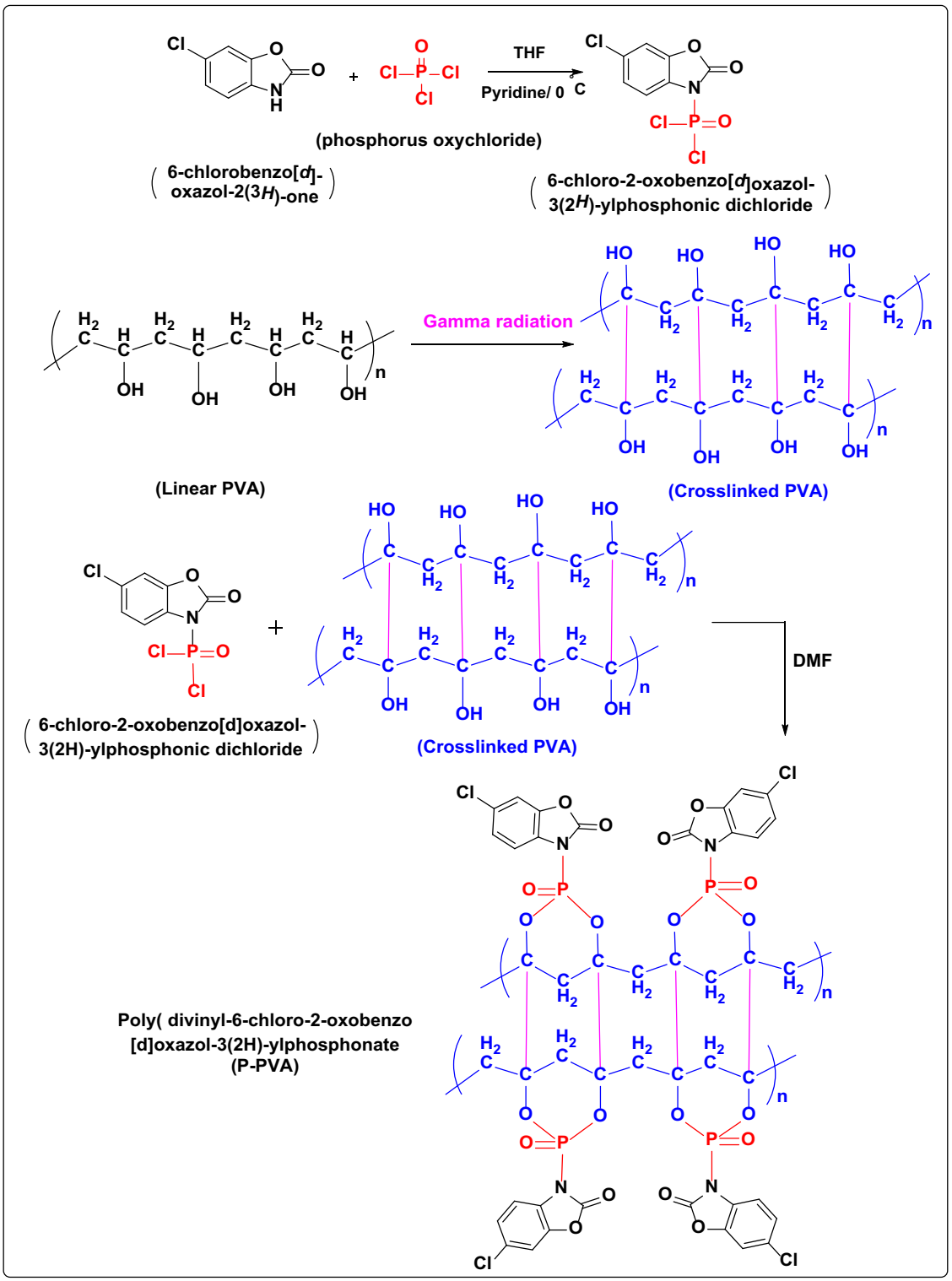


**Scheme 1** Synthesis of phosphorus-containing PVA

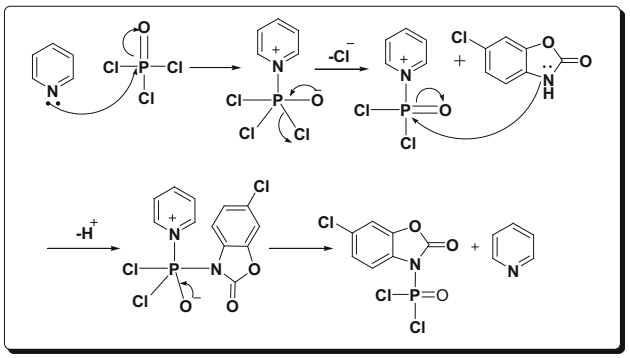

**Scheme 2** Mechanism for synthesis of 6-chloro-2-oxobenzo[d]oxazol-3(2H)-ylphosphonic dichloride


**Fig. 1** The photograph of neat PVA **a** and phosphorus–contained polymers; P-PVA **b**

confirm the presence of complexation between 6-chloro-2-oxobenzo [d] oxazol-3 (2H) -yl phosphonic dichloride and PVA matrix. Pure PVA shows typical vinyl polymer bands, 2800–3000 $cm^{-1}$ bands emerging due to stretching vibration of the CH and $CH_2$ groups, and bands attributed to $CH/CH_2$ deformation vibrations are present between 1300 $cm^{-1}$ and 1500 $cm^{-1}$ which shifted to higher values in the P-PVA spectrum. A broad weak absorption peak appeared between 3600 $cm^{-1}$ and 3000 $cm^{-1}$ which is characteristic of the stretching vibration of unreacted OH groups and accompanying C–O stretching exists between 1000 $cm^{-1}$ and 1260 $cm^{-1}$. Intensive C = O stretching vibrations are detected at 1750 $cm^{-1}$ [23]. The aromatic out-of-plane bends appeared at 760 $cm^{-1}$ and the band at 770–690 $cm^{-1}$ is due to ring deformation [24]. The presence of oxygen in all of the synthesized phosphorus-containing polymers is related to either incorporation of oxygen-containing organic radicals initiating polymerization into the polymer structure or partial oxidation of the surface layers of polymeric phosphorus. There are additional specific absorptions at a spectrum of phosphorus-containing polymer and not present in the PVA spectrum. This is reflected in the IR spectra as an expanding phosphorus-oxygen vibrator: 1180 $cm^{-1}$ (P = O), and 1030,

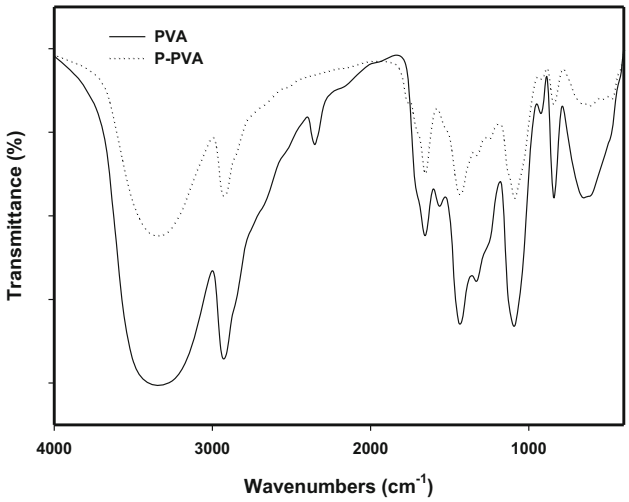


**Fig. 2** FTIR spectra of PVA and P-PVA at irradiation dose; 20 kGy

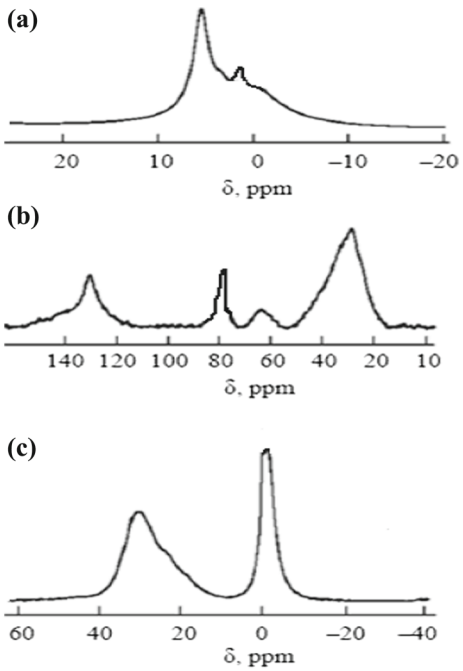


**Fig. 3** NMR spectra of phosphorus-containing polymer, **a** $^{1}H$ **b** $^{13}C$ **c** $^{31}P$

985 $cm^{-1}$ (P–O–C), indicating the presence of phosphonate groups hanging in the polymer chain [25].

Figure 3 shows $^{1}H$, $^{13}C$, and $^{31}P$ NMR spectra of the phosphorus-containing PVA. As can be seen, the proton spectrum (Fig. 3a) is composed of three parts: a strong signal at 5.5 ppm of protons at the double bonds. The nature of the spectrum confirms a region of the double bonds. The structure of the compound is much more mobile and uniform than aliphatic. This may suggest that the cross-linking is present in the aliphatic part of the compound at the points of binding with the double bonds. The δ values which ranged between

7.35–7.70 ppm and 3.90–4.31 ppm are due to aromatic protons and P–O–CH, respectively. The presence of a relatively pronounced signal at 3.7 ppm indicates that there are oxidized and/or chlorinated groups more mobile than the other aliphatic groups [26].

The $^{13}C$ NMR experiment was carried out using the technique of rotation at the magic angle with strong suppression of the dipole–dipole interactions on the frequency of the proton resonance and with the transfer of polarization from protons to the carbon nuclei. Without this technology, the accumulation is ineffective. It is obvious that the resulting spectrum has four broad signals: one belongs to the carbon in the double bond (~ 132 ppm) and the other, to the saturated aliphatic carbon atoms. From the overall spectrum pattern, we can conclude that the compound under study is disordered by the composition and structure (amorphous), with low mobility of all its components. Apparently, at room temperature the compound is in a state below its glass transition temperature or has a large number of cross-linking, or more likely, both reasons are valid [26]. Analysis of the chemical shift and shape of the signals suggests that the compound has components of butadiene –CH = CH– (~ 122 ppm) and > CH–$CH_2$– (29–34 ppm). Also, the carbon atoms are connected with oxygen, and phosphorus (Fig. 3b). The group CH–O–$PO_2$N is likely to be characterized by the shoulder in the range of 40–46 ppm of the main aliphatic signal (28.7 ppm) [26].

$^{31}P$ NMR spectrum confirms that the compound including > CH–O–$PO_2$N has a signal at ~ 0 to 1.4 ppm [27]. Since the mobility of the > CH–O–$PO_2$N groups is associated with the polymer via oxygen bridges (Fig. 3c). Thus the conclusion about the formation of cross-links involving carbon atoms directly adjacent to both types of groups obtained at the analysis of the $^{13}C$ NMR spectra is confirmed by the data of $^{31}P$ NMR spectroscopy.

### 3.3 EDX Measurements

To determine the identity of the phosphorus in the polymer, EDX was carried out. It is a characterization technique that provides an elemental composition of various constituent elements in a material. The abscissa of the EDX spectrum indicates the ionization energy and the ordinate indicates the counts. Quantitative elemental analysis of the P-PVA hydrogel was done through EDX studies; the results are shown in Fig. 4 and Table 1. The atomic % (weight %) of Carbon, Nitrogen, Oxygen, Phosphorus, and Chlorine was found to be 55.45% (54.66%), 5.15% (6.17%), 24.35% (23.19%), 8.20% (10.34%), and 6.85% (5.64%), respectively. In addition to these peaks, a small peak is also found at about 2.1 keV in the sample, which indicates the presence of Au which has been used as a sputter coating, while preparing the samples for the analysis [28]. The resulted elements by EDX support the suggested structure of P-PVA in Scheme 1.

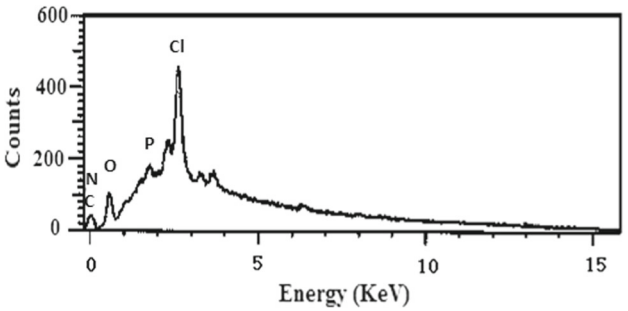


**Fig. 4** EDX pattern of the phosphorus-containing polymer

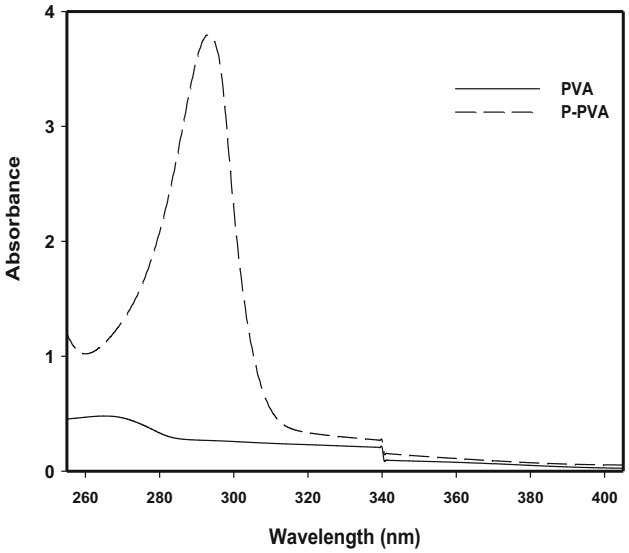


**Fig. 5** UV–Vis spectra of PVA and P-containing PVA at irradiation dose; 20 kGy

### 3.4 Ultraviolet Spectroscopy (UV)

The observed UV spectra, shown in Fig. 5, exhibit the following transitions. The absorption bands for γ-irradiated PVA and P-PVA hydrogels may be assigned to π- π* which comes from unsaturated bonds; mainly, C = O and/or C = C [29]. The spectra of PVA showed a sharp decrease in intensity at about 270 nm in comparison to P-PVA which has broadband at about 290 nm. Hence, the increased absorbance of P-PVA hydrogels indicates the presence of phosphorus in the hydrogel matrix. This leads to the shifting of the plasmon resonance band. This is due to the multipoles interaction inside the hydrogel matrix. On the other hand, plasmon absorption increment in the UV–spectra represents the formation of a phosphorus-containing polymer.

**Table 1** Comparison between the atomic and weight percentage of P-PVA hydrogels

| Sample | C atomic% (weight%) | N atomic% (weight%) | O atomic% (weight %) | P atomic% (weight %) | Cl atomic% (weight %) |
|---|---|---|---|---|---|
| P-PVA hydrogels | 55.45 (54.66) | 5.15 (6.17) | 24.35 (23.19) | 8.20 (10.34) | 6.85 (5.64) |

**Table 2** Gel content and degree of swelling of PVA and P-PVA polymers

| Hydrogel | Gel content (%) | Swelling (g/g) |
|---|---|---|
| PVA | 95 | 3.7 |
| PVA-P | 90 | 9.2 |

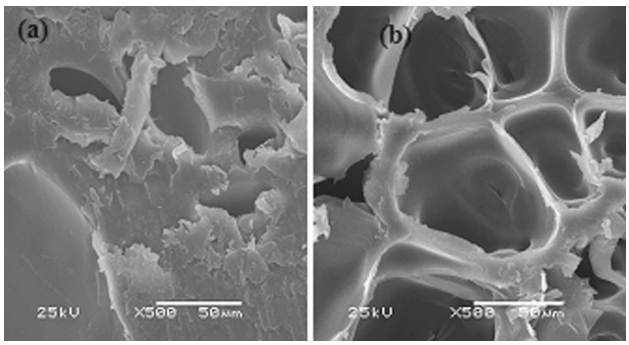


**Fig. 6** SEM of **a** PVA and **b** P-PVA hydrogels. Irradiation dose; 20 kGy

## 3.5 Gel Content and Swelling

The degree of crosslinking of polymers can be assessed by measuring the mass percentage of the gel fraction. The gel content and the crosslinking network density of PVA and P-PVA polymers have a significant impact on their swelling character. The gel content of PVA and P-PVA was shown in Table 2. The gel content of PVA hydrogel increases significantly less than P-PVA. Swelling behavior results showed that P-PVA hydrogel has more swelling properties than pure PVA with about a triple value. These results can be supported by studying the surface morphology of hydrogel surfaces by SEM. It was used to observe the micromorphology on fresh cross sections of hydrogel samples dehydrated by the freeze-dryer technique. The micromorphology of the prepared hydrogel as well as its pore diameter mainly depends on those factors affecting the swelling properties of hydrogels [30, 31]. The pore size and morphological structure of the PVA and P-PVA polymers were investigated and shown in Fig. 6. The P-PVA hydrogels show a larger pore structure than PVA, this leads to an accelerated swelling rate.

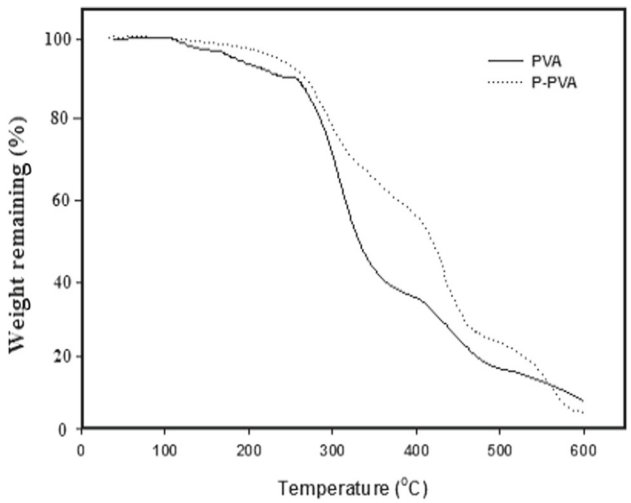


**Fig. 7** TGA plots of PVA and P-PVA hydrogels. Irradiation dose; 20 kGy

## 3.6 Thermal Properties

Thermal analysis of polymers was performed using DSC and TGA. The occurrence of intermolecular associations between PVA and phosphorus heterocyclic moiety can be measured by using TGA to demonstrate the thermal stability of polymers. Figure 7 shows a thermo-gravimetric diagram of PVA and P-PVA hydrogels at temperature intervals from 30 to 600 °C. TGA curves of PVA and P-PVA include three different areas of weight loss. The initial weight loss is in the range of 30–280 °C. This is due to the traces of moisture present. The second zone (280–400 °C) was due to the degradation of the polymer backbone. The third zone was above 400 °C. The thermal decomposition rate of P-PVA hydrogels relative to the temperature was slower than pure PVA. It is clear that the decomposition temperature required for the pure PVA is lower than that required for P-PVA hydrogels. It is concluded that the thermal stability of PVA was improved by adding phosphorus heterocyclic moiety [32, 33].

Figure 8 shows the thermal diagram of PVA and P-PVA hydrogels, whereas Table 3 shows their thermal parameters. It is clear that the Tm of PVA decreased with the incorporation of phosphorus-heterocyclic moiety whereas, ΔHm increased. The obtained results reflect the interactions between PVA and phosphorus-containing heterocyclic moiety.

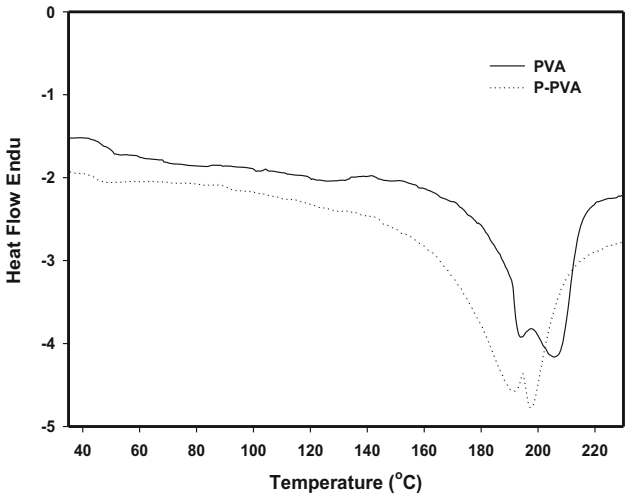


**Fig. 8** DSC diagram for PVA and P-PVA hydrogels. Irradiation dose; 20 kGy

**Table 3** Thermal parameters for PVA and P-PVA hydrogels

| Hydrogel | Tm (°C) | Δ Hm (J/g) |
|---|---|---|
| PVA | 205.8 | 62.2 |
| P-PVA | 197.4 | 77.5 |

## 3.7 Biological Studies

PVA and phosphorus-contained hydrogels; P-PVA were tested for antifungal and antibacterial activity against different fungal and bacterial strains. The antifungal strains include *Aspergillus fumigatus, Geotrichum candidum, Candida albicans,* and *Syncephal-astrum racemosum*. The samples were analyzed for the calculation of inhibited fungal zone and a comparative study of the results was done against the standard drugs; Itraconazole and Clotrimazole (Table 4). The antibacterial strains include *Staphylococcus aureus, Bacillis subtilis* (as gram-positive bacteria), *Pseudomonas aeruginosa,* and *Escherichia coli* (as gram-negative bacteria). The samples were analyzed for the calculation of inhibited bacterial zone and a comparative study of the results was done against the standard drugs; Penicillin G and Streptomycin (Tables 5) [28].

The zone of fungal growth inhibition for the standard Itraconazole drug was found to be 28 ± 0.05 mm, 27 ± 0.10 mm, 26 ± 0.02 mm, and 22 ± 0.09 mm against *Aspergillus fumigatus, Geotrichum candidum, Candida albicans,* and *Syncephal-astrum racemosum*, respectively. Also, the zone for the standard Clotrimazole drug was found to be 26 ± 0.10 mm, 23 ± 0.03 mm, 18 ± 0.10 mm, and 20 ± 0.20 mm, respectively. In the case of PVA hydrogels, they were found to possess antifungal activity only in the case of *Aspergillus fumigatus, Geotrichum candidum,* and *Candida albicans.* The zone of fungal growth inhibition was found to be 11.2 ± 0.03 mm, 13.4 ± 0.04 mm, and 10.2 ± 0.03 mm, respectively. P-PVA hydrogels possess antifungal activity in the case of *Aspergillus fumigatus, Geotrichum candidum,* and*Candida albicans with* 15.2 ± 0.06 mm, 18.4 ± 0.04 mm, and 15.4 ± 0.1 mm, respectively. The results proved that P-PVA hydrogels possess higher antifungal activity compared to PVA samples.

The zone of bacterial growth inhibition for the standard Penicillin G drug was found to be 29.4 ± 0.08 mm, 32.5 ± 0.05 mm, 28.3 ± 0.10 mm, and 33.5 ± 0.07 mm against *Staphylococcus aureus, Bacillis subtilis*, *Pseudomonas aeruginosa,* and *Escherichia coli*, respectively. Also, the zone for the standard Streptomycin drug was found to be 5 ± 0.20 mm, 29 ± 0.04 mm, 24 ± 0.10 mm, and 25 ± 0.03 mm, respectively. PVA hydrogels were found to possess antibacterial activity only in the case of *Staphylococcus aureus,* and *Bacillis subtilis* with 14.40 ± 0.50 mm, 16.40 ± 0.10 mm, respectively. P-PVA hydrogels possess antibacterial activity for all bacterial strains. The zone of bacterial growth inhibition was found to be 7.20 ± 0.01 mm, 18.30 ± 0.03 mm, 11.40 ± 0.09 mm, and 9.20 ± 0.02 mm, respectively [34, 35]. The results showed that the antibacterial activity of P-PVA hydrogels was found to possess higher antibacterial activity compared to PVA samples.

A schematic mechanism of the antimicrobial activity is depicted in Fig. 9. Antimicrobial activity can be divided into active polymers and passive polymers. Active polymers actively kill bacteria that adhere to the polymer surface. Polymers functionalized with active agents, such as cationic biocides, antimicrobial peptides, or antibiotics, can kill bacteria on contact. The mechanism of polymers killing microbes depends on the active agents. The highly active antimicrobial polymers act positively-charged quaternary ammonium, interacting with the cell wall and destroying the cytoplasmic membrane, leading to leakage of intracellular segments and subsequent cell death [36]. A passive polymer layer can reduce protein adsorption on its surface, thereby preventing bacterial adhesion. However, although passive surfaces repel bacteria, they do not actively interact with or kill bacteria. Due to the mainly hydrophobic and negatively-charged properties of microbes, passive polymers should be either (1) Hydrophilic; (2) Negatively charged; or (3) Have a low surface free energy (Fig. 9) [37, 38]. Typical passive polymers include (1) Self-healing, slippery liquid-infused porous surface, such as poly(dimethyl siloxane); (2) Uncharged polymers, such as poly(ethylene glycol) (PEG), poly(2-methyl-2-oxazoline), polypeptide, poly(n-vinyl-pyrrolidone), and poly(dimethyl acrylamide); and (3) Charged polyampholytes and zwitterionic polymers, such as phosphobetaine, sulfobetaine, and phospholipid polymers [39, 40]. PEG has been the most commonly used passive

**Table 4** Antifungal activity data of the tested hydrogels

| Compounds | Inhibition zone diameter (mm) | | | |
|---|---|---|---|---|
| | *Aspergillus fumigatus* (RCMB 002003) | *Geotrichum candidum* (RCMB 052006) | *Candida albicans* (RCMB 005002) | *Syncephal-astrum racemosum* (RCMB 005003) |
| PVA | 11.2 ± 0.03 | 13.4 ± 0.04 | 10.2 ± 0.03 | NA |
| P-PVA | 15.2 ± 0.06 | 18.4 ± 0.04 | 15.4 ± 0.10 | NA |
| *Itraconazole* | 28.0 ± 0.05 | 27.0 ± 0.10 | 26.0 ± 0.02 | 22.0 ± 0.09 |
| *Clotrimazole* | 26.0 ± 0.10 | 23.0 ± 0.03 | 18.0 ± 0.10 | 20.0 ± 0.20 |

Mean zone of inhibition in mm ± Standard deviation beyond well diameter (6 mm) produced on a range of environmental and clinically pathogenic microorganisms using (10 mg/ml) concentration of tested samples and standard using (30 µg/ml)
The test was done using the diffusion agar technique, Well diameter: 6.0 mm (100 µl was tested)
*NA* No activity, data are expressed in the form of mean ± SD

**Table 5** Antibacterial activity data of the tested hydrogels

| Compounds | Inhibition zone diameter (mm) | | | |
|---|---|---|---|---|
| | Gram positive bacteria | | Gram negative bacteria | |
| | *Staphylococcus aureus* (RCMB 000106) | *Bacillis subtilis* (RCMB 000107) | *Pseudomonas aeruginosa* (RCMB 000102) | *Escherichia coli* (RCMB 000103) |
| PVA | 14.4 ± 0.50 | 16.4 ± 0.10 | NA | NA |
| P-PVA | 7.2 ± 0.01 | 18.3 ± 0.03 | 11.4 ± 0.09 | 9.2 ± 0.02 |
| Penicillin G | 29.4 ± 0.08 | 32.5 ± 0.05 | 28.3 ± 0.10 | 33.5 ± 0.07 |
| Streptomycin | 5.0 ± 0.20 | 29.0 ± 0.04 | 24.0 ± 0.10 | 25.0 ± 0.03 |

Mean zone of inhibition in mm ± Standard deviation beyond well diameter (6 mm) produced on a range of environmental and clinically pathogenic microorganisms using (10 mg/ml) concentration of tested samples and standard using (30 µg/ml)
The test was done using the diffusion agar technique, Well diameter: 6.0 mm (100 µl was tested)
*NA*: No activity, data are expressed in the form of mean ± SD

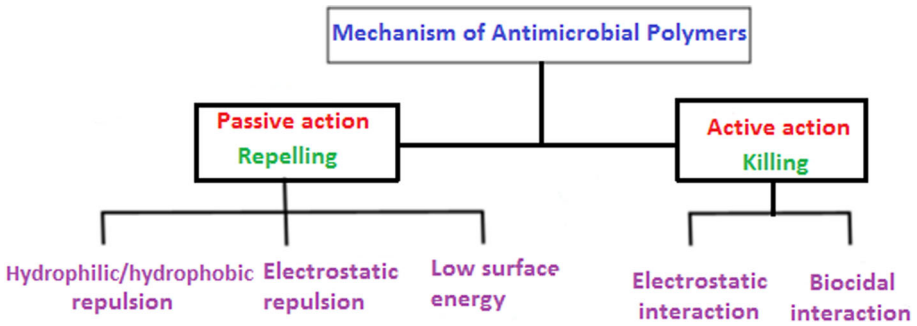


**Fig. 9** The schematic reaction mechanisms of passive and active action of the antimicrobial polymers

antimicrobial material [41], and studies have shown that it exhibits a high antifouling ability to prevent protein and cell adhesion effectively, consequently preventing the growth of microbes. Among these passive polymers; P-PVA is studied here. It has been extensively and has demonstrated excellent antimicrobial effects in drastically reducing protein adsorption and bacterial adhesion. Due to high hydrophilicity, high chain mobility, large exclusion volume, and steric hindrance effect of highly hydrated layer [38].

## 4 Conclusions

Phosphorus-containing polymer was synthesized by reaction of radiation-induced crosslinked polyvinyl alcohol with phosphorus-heterocyclic moiety. The gel content of PVA hydrogel increased significantly less than that of PVA containing phosphorus heterocyclic moiety. Swelling behavior results have shown that P-PVA hydrogel has more swelling properties than pure PVA with about a triple value. EDX analysis of P-PVA showed that Carbon, Nitrogen, Oxygen,

Phosphorus, and Chlorine were found in hydrogel sample. Plasmon absorption increment in the UV–spectra represents the formation of a phosphorus-containing polymer. Thermal analysis of polymers proved that the thermal decomposition rate of P-PVA hydrogels in terms of temperature was slower than pure PVA. The Tm of PVA decreased with incorporating phosphorus-heterocyclic moiety, whereas ΔHm increased. Antifungal ability can be significantly enhanced in P-PVA hydrogels compared to PVA ones. For in vitro fungal and bacterial adhesion, studies have shown significant differences between pure PVA gel and P-PVA which have shown high inhibition. It is concluded that phosphorus-based polymers are suitable for many different medical applications such as drug delivery and wound healing.

**Funding** Open access funding provided by The Science, Technology & Innovation Funding Authority (STDF) in cooperation with The Egyptian Knowledge Bank (EKB).



## References

1. Ashfaq, A.; Clochard, M.-C.; Coqueret, X.; Dispenza, C.; Driscoll, M.S.; Ulański, P., et al.: Polymerization reactions and modifications of polymers by ionizing radiation. Polymers **12**, 2877–2884 (2020)
2. Amol, T.N.; Bhuwanesh, K.S.; Keyur, D.B.; Prakash, A.M.: Gamma radiation processed polymeric materials for high performance applications: a review. Front. Chem. **10**, 1–15 (2022)
3. Muhammad, A.; Rahman, M.R.; Baini, R.; Bin Bakri, M.K.: Applications of sustainable polymer composites in automobile and aerospace industry. **185**, 207- 215 (2021).
4. Sharma, B.K.; Krishnanand, K.; Mahanwar, P.A.; Sarma, K.S.S.; Ray, C.S.: Gamma radiation aging of EVA/EPDM blends: effect of vinyl acetate (VA) content and radiation dose on the alteration in mechanical, thermal, and morphological behavior. J. Appl. Polym. Sci. **135**, 46216–46225 (2018)
5. Darwis, D.; Erizal, B.; Abbas, B.; Nurlidar, F.; Putra, D.P.: Radiation processing of polymers for medical and pharmaceutical applications. Macromol. Symp. **353**, 15–23 (2015)
6. Davenas, J.; Stevenson, I.; Celette, N.; Cambon, S.; Gardette, J.L.; Rivaton, A., et al.: Stability of polymers under ionising radiation: the many faces of radiation interactions with polymers. Res. Sect. B Beam Interact. Mater. At. **191**, 653–661 (2002)
7. Dawes, K.; Glover, L.C.; Vroom, D.A.: The effects of electron beam and g -irradiation on polymeric materials. Physical Properties of Polymers Handbook, Second Edition, vol. 867–887 (2022).
8. Sun, Z.; Song, C.; Wang, C.; Hu, Y.; Wu, J.: Hydrogelbased controlled drug delivery for cancer treatment: a review. Mol. Pharm. **17**(2), 373–391 (2020)
9. Husain, M.S.B.; Gupta, A.; Alash, B.Y.; Sharma, S.: Synthesis of PVA/PVP based hydrogel for biomedical applications: a review. Energy Sources, Part A Recover. Util. Environ. Eff. **40**(20), 2388–2393 (2018)
10. Jiang, Y.; Hou, Y.; Fang, J., et al.: Preparation and characterization of PVA/SA/HA composite hydrogels for wound dressing. Int. J. Polym. Anal. Charact. **24**, 132–141 (2019)
11. Tafahom, A.J.; Asrar, A.S.: Effect of gamma irradiation on the physical properties of PVA polymer. Mater. Sci. Eng. **928**, 072137–072153 (2020)
12. Kumaraswamy, S.; Mallaiah, S.H.: Swelling and mechanical properties of radiation crosslinked Au/PVA hydrogel nanocomposites. Radiat. Eff. Defects Solids **171**(11–12), 869–878 (2016)
13. Kamoun, E.A.; Kenawy, E.S.; Chen, X.: A review on polymeric hydrogel membranes for wound dressing applications: PVA-based hydrogel dressings. J. Adv. Res. **8**(3), 217–233 (2017)
14. Wenbo, Z.; Sichun, L.; Jianzhong, M.; Yingke, W.; Chao, L.; Hongxia, Y.: pH-Induced electrostatic interaction between polyacrylates and amino-functionalized graphene oxide on stability and coating performances. Polymers **13**, 34063–34075 (2021)
15. Somasundarana, D.; Guhanathanb, S.: Organo phosphorous 3, 4-Dihydro-2 (H) –Pyrimidinone functionalised vinyl polymer – synthesis and characterisation. Int. J. Front. Sci. Technol. **3**(1), 10–24 (2015)
16. Zhangyong, Si.; Wenbin, Z.; Dicky, P.J.; Li, C.H.K.; En-Tang, K.; Kevin, P.; Mary, B.C.: Polymers as advanced antibacterial and antibiofilm agents for direct and combination therapies. Chem. Sci. **13**, 345–358 (2022)
17. Xu, J.P.; Liu, Y.; Hsu, S.H.: Hydrogels based on Schiff base linkages for biomedical applications. Molecules **24**(16), 3005–3014 (2019)
18. Ouyang, J.; Liu, R.Y.; Chen, W.; Liu, Z.; Xu, Q.; Zeng, K.; Liu, Y.N.: A black phosphorus based synergistic antibacterial platform against drug resistant bacteria. J. Mater. Chem. B **6**, 6302–6310 (2018)
19. Xu, L.-C.; Li, Z.; Tian, Z.; Chen, C.; Allcock, H.R.; Siedlecki, C.A.: A new textured polyphosphazene biomaterial with improved blood coagulation and microbial infection responses. Acta Biomater. **67**, 87–98 (2018)
20. Alvin, K.R.G.; Lorna, S.R.; Alyan, P.S.: Gel properties of carboxymethyl hyaluronic acid/polyacrylic acid hydrogels prepared by electron beam irradiation. Mater. Proc. **7**(1), 13–21 (2021)
21. Relleve, L.S.; Gallardo, A.K.R.; Abad, L.V.: Radiation crosslinking of carboxymethyl hyaluronic acid. Radiat. Phys. Chem. **151**, 211–216 (2018)
22. Lim, Y.H.; Tiemann, K.M.; Heo, G.S.; Wagers, P.O.; Rezenom, Y.H.; Zhang, S.; Zhang, F.; Youngs, W.J.; Hunstad, D.A.; Wooley, K.L.: Preparation and in vitro antimicrobial activity of silver-bearing degradable polymeric nanoparticles of Polyphosphoester-block-Poly(l-lactide). ACS Nano **9**, 1995–2008 (2015)
23. Bock, P.; Gierlinget, N.; Socrates, G.: Infrared and raman spectra of lignin substructures: Coniferyl alcohol, abietin, and coniferyl aldehyde. J. Raman Spectrosc. (2019). https://doi.org/10.1002/jrs.5588
24. Chai, J.; Zhang, K.; Xue, Y.; Liu, W.; Chen, T.; Lu, Y.; Zhao, G.: Review of MEMS based fourier transform spectrometers. Micromachines **11**, 214–241 (2020)
25. Ahmed, F.; Diana, P.; Vitor, H.; Carvalho, S.O.C.; Graça, M.: Fourier transform infrared (FTIR) spectroscopy to analyse human blood over the last 20 years: a review towards lab-on-a-chip devices. Micromachines **13**, 187–206 (2022)

26. Kay, Saalwächter: Chapter 1: applications of NMR in polymer characterization – an introduction, In: NMR methods for characterization of synthetic and natural polymers. Royal Sci. Chem. pp. 1–22 (2019).
27. Rajini, A.; Muralasetti, N.; Kaliaperumal, S.; Ingala, A.; Venkatathri, N.: A novel vanadium n-propylamino phosphate catalyst: synthesis, characterization and applications. Mater. Res. **16**(1), 181–189 (2013)
28. Sharma, A.K.; Kaith, B.S.; Gupta, B.; Shanker, U.; Locha, S.P.: A facile strategy to synthesize a novel and green nanocomposite based on gum Salai guggal - Investigation of antimicrobial activity. Mater. Chem. Phys. **219**, 129–141 (2018)
29. Shujing, P.; Zhiqiang, G.; Jie, S.; Lan, L.; Chunxia, W.; Yiping, Q.: Influence of absorbed moisture on solubility of poly(vinyl alcohol) film during atmospheric pressure plasma jet treatment. Surf. Coat. Tech. **15**, 1222–1228 (2010)
30. Abd El-Mohdy, H.L.: Functional modification of poly vinyl alcohol/acrylic acid hydrogels prepared by γ-radiation through some amine compounds. Arab. J. Chem. **10**, S431–S438 (2017)
31. Abd El-Mohdy, H.L.; Tahia, B.M.: Synthesis of polyvinyl alcohol/maleic acid hydrogels by electron beam irradiation for dye uptake. J Macromol. Sci. Part A Pure Appl. Chem. **50**, 6–17 (2013)
32. Tretsiakova-McNally, S.; Joseph, P.: Thermal and calorimetric evaluations of polyacrylonitrile containing covalently-bound phosphonate groups. Polymers **10**, 131–137 (2018)
33. Sun, Y.; Wang, Y.; Liu, L.; Xiao, T.: The preparation, thermal properties, and fire property of a phosphorus-containing flame-retardant styrene copolymer. Materials **13**, 127–133 (2020)
34. Sharma, A.K.; Kaith, B.S.; Shanker, U.; Gupta, B.: γ-radiation induced synthesis of antibacterial silver nanocomposite scaffolds derived from natural gum Boswellia serrata. J. Drug Deliv. Sci. Technol. **56**, 101550–101563 (2020)
35. Sharma, A.K.; Kaith, B.S.; Gupta, B.; Shanker, U.; Locha, S.P.: Microwave assisted in situ synthesis of gum Salai guggal based silver nanocomposites- investigation of anti-bacterial properties. Cellulose **26**, 991–1011 (2019)
36. Xue, Y.; Xiao, H.; Zhang, Y.: Antimicrobial polymeric materials with quaternary ammonium and phosphonium salts. Int. J. Mol. Sci. **16**, 3626–3655 (2015)
37. Francolini, I.; Donelli, G.; Crisante, F.; Taresco, V.; Piozzi, A.: Antimicrobial polymers for anti-biofilm medical devices: state-of-art and perspectives. Adv. Exp. Med. Biol. **831**, 93–117 (2015)
38. Zhang, H.; Chiao, M.: Anti-fouling coatings of poly(dimethylsiloxane) devices for biological and biomedical applications. J. Med. Biol. Eng. **35**, 143–155 (2015)
39. Liu, L.; Li, W.; Liu, Q.: Recent development of antifouling polymers: structure, evaluation, and biomedical applications in nano/micro-structures. WIREs Nanomed. Nanobiotechnol. **6**, 599–614 (2014)
40. Ye, Q.; Zhou, F.: Antifouling surfaces based on polymer brushes. In: Zhou, F. (Ed.) Antifouling surfaces and materials, pp. 55–81. Springer, Berlin, Germany (2015)
41. Yu, K.; Mei, Y.; Hadjesfandiari, N.; Kizhakkedathu, J.N.: Engineering biomaterials surfaces to modulate the host response. Colloids Surf. B Biointerfaces **124**, 69–79 (2014)